Integrated Computation of Micro-Cavitation in Gasoline Injector Atomization

Jun Ishimoto*
Institute of Fluid Science, Tohoku University
Sendai 980-8577, Japan

Abstract

The effect of micro-cavitation on 3-D structure of liquid atomization process through a gasoline injector nozzle is numerically investigated and visualized by a new type of integrated CFD technique. The present CFD analysis focused on primary breakup phenomenon of a liquid column which is closely related to the micro-cavitation, the consecutive formation of liquid film, and generation of droplets of a lateral flow in the outlet section of the nozzle. The governing equations for high-speed lateral atomizing injector nozzle flow taking into account the micro-cavitation generation based on the Barotropic LES-VOF model in conjunction with the CSF model are presented, and then an integrated parallel computation are performed to clarify the detailed atomization process coincident with the micro-cavitation of a high speed nozzle flow. Furthermore, we acquire the data which is difficult to confirm by experiment such as aspects and volume fraction of micro-cavity, liquid core shapes, spray angle and spray velocity profiles.

Introduction

Micro-cavitation can be thought of as slight vaporization induced by flow generated local pressure drop and the region of vapor may be large continuous bubbly cloud. Therefore, Micro-cavitation in high-speed flow as in gasoline injectors is almost-isothermal but compressibility effects may be important particularly if the cavitation is unstable and vapor bubbles enter the liquid core and collapse causing pressure waves to interfere/enhance the liquid jet. At the present, a little amount of CFD study of the nozzle jet flow with cavitation have been performed. Main results of these research are listed as; a numerical model that treats liquid and vapor as a continuum has been constructed for predicting small scale, high speed, cavitating, nozzle flow by Schmidt [1]; the coupled standard discrete droplet model, conventional breakup model, and the Eulerian multi-fluid model are applied to analyze cavitating nozzle flow by Berg [2]; 2-D simulation of the strong interaction of cavitating nozzle flow with the outside jet formation was performed and the direct interaction between the cavitation and the jet are analyzed by Yuan [3]. However, those research have not enough focused on turbulent primary breakup phenomenon, and also their used numerical model of conventional type does not have sufficient high resolution to analyze primary breakup phenomenon. As their model does not have accurate turbulence model such as LES yet, it has possessed the limit to analyze micro-scale turbulent atomization.

The present integrated CFD analysis focused on the detailed behavior of the micro-cavitation generation in gasoline injector nozzle. The computation is performed especially in the primary breakup phenomenon of a liquid column including that in the upstream of aperture region, which is closely related to the micro-cavitation generation, the consecutive formation of liquid film, and generation of droplets of a lateral high-speed turbulent flow in the outlet section of the nozzle.

Governing equations for Continuum Barotropic Models for Cavitation

The basis of the Continuum Barotropic approach for cavitation is the compressible mixture form of continuity and momentum equations. It comprises a single set of conservation equations for the whole flow field even though fluid properties are discontinuous across the fluid boundaries. These equations are written as follows.

*Corresponding author, E-mail: ishimotojun@ieee.org

The mass conservation equation:

$$\frac{\partial \rho}{\partial t} + \nabla \cdot (\rho \boldsymbol{v}) = 0, \tag{1}$$

Momentum equation:

$$\begin{aligned} &\frac{\partial}{\partial t}(\rho \boldsymbol{v}) + \nabla \cdot (\rho \boldsymbol{v}\boldsymbol{v}) \\ &= -\nabla p + \nabla \cdot \boldsymbol{\tau} + \int_{S(t)} \sigma \kappa' \boldsymbol{n}' \delta (\boldsymbol{x} - \boldsymbol{x}')\, dS. \end{aligned} \tag{2}$$

The closure of basic equations requires an equation of state described as follow.

$$\rho = f(p). \tag{3}$$

A common Barotropic model used for cavitation is based on the non-equilibrium equation is derived as follows.

$$\frac{\mathrm{D}\rho}{\mathrm{D}t} = \frac{1}{a^2}\frac{\mathrm{D}p}{\mathrm{D}t}, \tag{4}$$

where a is the velocity of pressure waves (the sound velocity) in the cavitating mixture. This equation can be integrated analytically between liquid and vapor states as in the work of Schmidt [1] to obtain an equation of state in standard form $p = f(\rho)$ but this leads to a potential inconsistency between the mixture and liquid/vapor equations of state. Alternatively Eq. 4 could be used directly with the mixture continuity equation to formulate a pressure equation. This approach has proved problematic because the non-equilibrium nature of the closure means the mixture pressure and density are not consistent with liquid or vapor equations of state until equilibrium is attained and even then numerical errors may accumulate resulting in inconsistencies even at equilibrium. To avoid these difficulties a new equilibrium Barotropic model is proposed in which the pressure and density are guaranteed to obey the liquid and vapor equations of state in the limits and a mixture compressibility model in between. Simple linear model for the vapor and liquid equations of state are introduced as follow:

$$\rho_v = \psi_v p, \tag{5}$$

$$\rho_l = \rho_l^0 + \psi_l p. \tag{6}$$

The cavitation vapor-phase fraction obtained from the mixture density and the saturation conditions are introduced as follow:

$$\gamma = \max\left[\min\left(\frac{\rho_l^{\mathrm{sat}} - \rho}{\rho_l^{\mathrm{sat}} - \rho_v^{\mathrm{sat}}}, 1\right), 0\right], \tag{7}$$

and if the mixture density is obtained from the equilibrium equation of state:

$$\rho = (1-\gamma)\,\rho_l^0 + \left[\gamma\psi_v + (1-\gamma)\,\psi_l\right] p^{\mathrm{sat}} + \psi(\gamma)\left(p - p^{\mathrm{sat}}\right), \tag{8}$$

where $\psi(\gamma)$ is the mixture compressibility then in the limit of γ approaches to 1, the mixture density ρ will obey Eqn. (6) provided $\psi(\gamma) \to \psi_v$ and in the limit $\gamma \to 0$ the mixture density ρ will obey Eqn. (6) provided $\psi(\gamma) \to \psi_l$.

Basic equations for immiscible fluids

The numerical model represents the simultaneous unsteady flow of two immiscible, incompressible fluids, each having a constant viscosity and including surface tension. The LES-VOF equations are derived from Eq. (2) through a localized volume averaging of the phase weighted properties [4].

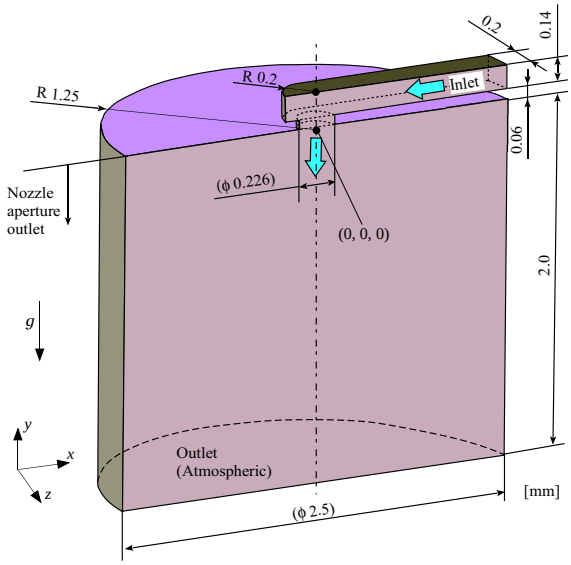

(a) Computational domain and geometry

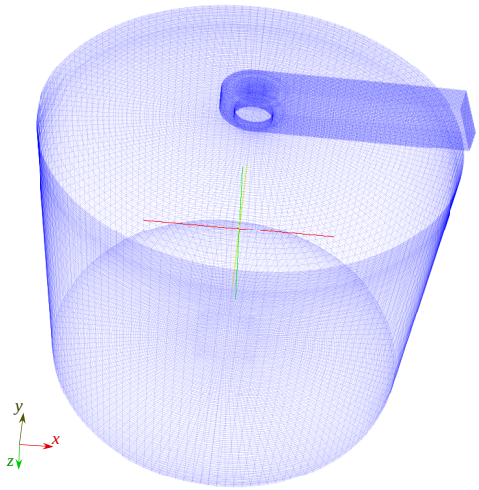

(b) Used computational mesh

Figure 1. Computational system of integrated CFD

Table 1. Numerical conditions

Nozzle aperture diameter	d	2.26×10^{-4}	m
Liquid-phase density	ρ_l	732.0	kg/m^3
Gas-phase density	ρ_g	1.134	kg/m^3
Inlet pressure	$p_{l(\mathrm{in})}$	0.444	MPa
Outlet pressure	$p_{l(\mathrm{ex})}$	0.101	MPa
Liquid-phase dynamic viscosity	μ_l	4.42×10^{-4}	$Pa \cdot s$
Gas-phase dynamic viscosity	μ_g	1.51×10^{-5}	$Pa \cdot s$
Surface tension	σ_l	0.0198	N/m

This process is more commonly known as filtering because it removes the very small scales of motion from direct calculation. The flow is considered to be a laminar incompressible Newtonian and isothermal flow and governed by the Navier-Stokes equations and continuity equations as shown in Eqs. (1) and (2). During the numerical solution process, we apply the free-surface boundary conditions. There are three hydrodynamic boundary conditions at free surfaces: normal stress balance, tangential stress balance, and the kinematic equation. The kinematic condition is implied by the VOF advection. The surface integral momentum equation represents the surface tension, therefore, cannot be calculated directly. Brackbill et al. [5] overcame this problem with their continuum surface force (CSF) model, which represents the surface tension effects as a continuous volumetric force acting within the transition region. For the turbulence modeling, LES of k-equation eddy-viscosity model is used [6]. The effect of the subgrid scale on the resolved eddies in momentum is represented by the SGS stress since it represents the effect of the unresolved small scale of turbulence. The geometry of the computational domain and the generated mesh are shown in Fig. 1. The numerical conditions are summarized in Table 1.

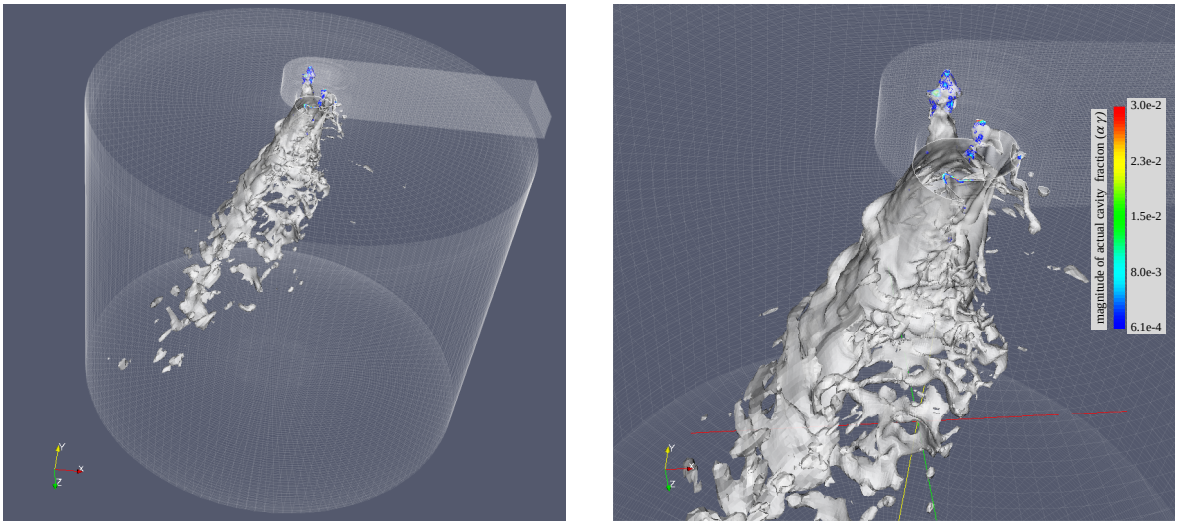

(a) t = 9.1e-4 s (b) t = 9.1e-4 s (close-up view)

Figure 2. Overview of the instantaneous iso-contour of the actual cavity fraction (vapor-phase fraction) $\alpha\gamma$ along with the liquid-vapor phase volume fraction of $\alpha = 0.5$. The color graduation represents the scalar magnitude of cavity fraction $\alpha\gamma$.

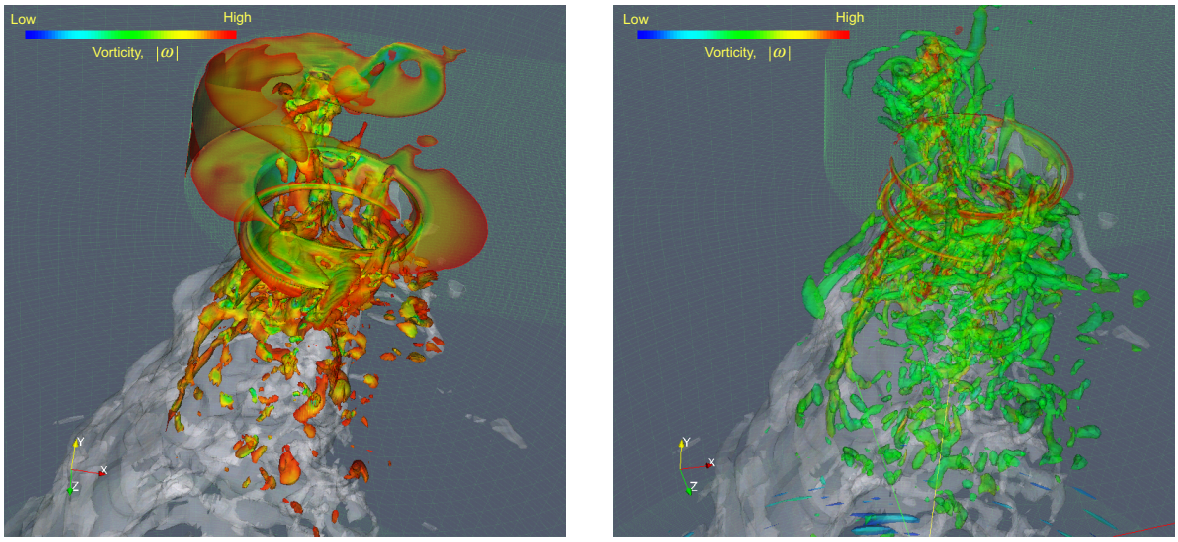

(a) enstrophy E, (t = 9.1e-4 s) (b) second invariant Q, (t = 9.1e-4 s)

Figure 3. Instantaneous iso-surface of (a) the enstrophy E, and (b) the second invariant of velocity gradient tensor Q profiles just inside and downstream of the nozzle

Results and discussions

Figure 2 shows the instantaneous iso-contour of the actual cavity fraction (vapor-phase fraction) $\alpha\gamma$ along with liquid-vapor phase volume fraction α. The threshold of the volume fraction is $\alpha = 0.5$ (gas-liquid interface). The color graduation represents the scalar magnitude of cavity fraction $\alpha\gamma$. With CFD analysis, it is possible to clearly elucidate the micro-cavitation behavior and atomization mechanism upstream of the nozzle aperture, which is invisible by visualization measurement. It is found that the micro-cavitation is quite locally generated at the edge of the nozzle aperture and also generated at the portion where the curvature of the liquid-phase fraction iso-surface becomes large. As the vapor pressure of gasoline is relatively large, micro-cavity is easily generates in spite of the low velocity conditions. When the liquid film is stretched, whose thickness becomes thin and the fluid velocity inside the thin liquid film layer increases prior to turn off, the micro-cavitation generates in that portion due to the local pressure drop. With time, a tornado like small swirling flow is locally generated from the aperture toward the upstream, the micro-cavitation is actively generated especially around the center of micro-vortex in the swirl. The vapor fraction of the micro-cavitation increases with increase in the magnitude of vortex. The magnitude of the micro-cavitation is mainly controlled by the amount of local pressure decrease closely related with the increase of scalar magnitude of the radial component of liquid-phase velocity. Especially in the center of the small swirling vortex, as the magnitude of velocity becomes large, it is found that the vapor fraction of cavity increases with decrease in local static pressure.

Figure 3 shows the iso-surface of the enstrophy E and the second invariant of velocity gradient tensor Q profiles just inside and downstream of the nozzle, respectively. The color graduation in both figures represents the scalar magnitude of vorticity, $|\boldsymbol{\omega}|$. According to Fig. 3, especially in the upstream portion of the nozzle aperture where the tornado-like micro-cavitation is actively generated, the vertical eddy toward the mainstream are created. It is found that the vertical turbulent vortices are elongated in the vortex-azimuthal direction due to the small-scaled swirling flow.

It is speculated that the contribution of the turbulent eddy generation is attained by the interference between the micro-cavity and the shear layer at the small-scaled swirling region. The numerical conditions are summarized in Table 1.

Conclusions

It was possible to accurately simulate complex two-phase atomizing gasoline injector nozzle flow with break-up, coalescence, compressibility effects and even the interaction between unstable cavitation and the free-surface. As a result, it was found that the micro-cavitation is quite locally generated at the edge of the nozzle aperture and also generated at the portion where the curvature of the liquid-phase fraction iso-surface becomes large. Furthermore, found that when the liquid film is stretched, whose thickness becomes thin and the fluid velocity inside the thin liquid film layer increases prior to turn off, the micro-cavitation generates in that portion due to the local pressure drop.

Nomenclature

a	sound velocity.
$\dfrac{\mathrm{D}}{\mathrm{D}t}$	substantial derivative.
p	absolute pressure.
t	time.
$\boldsymbol{v}$	vector of velocity.
γ	cavitation vapor-phase fraction.
ρ	density.
ψ	compressibility.
σ	surface tension coefficient.
$\boldsymbol{\omega}$	vector of vorticity.

Subscripts and superscripts.

$(\ )_g$	gas-phase.
$(\ )_l$	liquid-phase.

$(\ )_{lv}$	liquid-vapor mixture phase.
$(\ )^{\mathrm{sat}}$	saturation condition.
$(\ )_v$	vapor-phase.
$(\ )^0$	initial stationary state.

References

1. Schmidt, D. P., Rutland, C. J., and Corradini, M. L., "A fully compressible model of small, high speed, cavitating nozzle flows," *Atomization and Sprays* 9: 255–276 (1999).

2. von Berg, E., Edelbauer, W., Alajbegovic, A., Tatschl, R., Volmajer, M., Kegl, B., and Ganippa, L. C., "Coupled simulations of nozzle flow, primary fuel jet breakup, and spray formation," *Trans. ASME, J. Eng. Gas Turbines and Power* 127: 897–908 (2005).

3. Yuan, W. and Schnerr, G. H., "Numerical simulation of two-phase flow in injection nozzles: Interaction of cavitation and external jet formation," *Trans. ASME, J. Fluids Eng.* 125: 963–969 (2003).

4. Weller, H. G. and Tabora, G., "A tensorial approach to computational continuum mechanics using object-oriented techniques," *Computers in Physics* 12: 620–631 (1998).

5. Brackbill, J. U., Kothe, D. B., and Zemach, C., "A continuum method for modeling surface tension," *J. Comput. Phys.* 100: 335–354 (1992).

6. Ishimoto, J., Ohira, K., Okabayashi, K., and Chitose, K., "Integrated simulation of the atomization process of a liquid hydrogen jet through a cylindrical nozzle," *Cryogenics* 48: 238–247 (2008).